Temperature dependence of the ^{19}F transferred hyperfine interaction in the EPR of Mn^{2+}:PbF_2

M. Madrid, A. R. King, and V. Jaccarino
Department of Physics, University of California at Santa Barbara, Santa Barbara, California 93106
(Received 25 October 1984)

The EPR of Mn^{2+} in PbF_2 has been reexamined in an attempt to resolve the apparent discrepancy between the values of the ^{19}F transferred hyperfine structure (hfs) $A_{||}^{19}$ and $A_{\perp}^{19}$ previously observed in EPR measurements made between 77 and 300 K with those obtained from NMR studies below 2 K. Between 77 and 50 K the EPR is found to broaden, and the ^{19}F transferred hfs undergoes an abrupt change below $\sim$50 K suggesting that a local lattice distortion occurs. Below $\sim$20 K a well-resolved transferred hfs reappears. The high- and low-temperature values of $A_{||}^{19}$ and $A_{\perp}^{19}$ now agree with the aforementioned EPR and NMR results.

I. INTRODUCTION

Magnetic impurities have been introduced into the superionic conductor PbF_2 as a tool to study the motion of the F^- anion carrier.[1-4] When a Mn^{2+} impurity substitutionally replaces a Pb^{2+} in PbF_2, a strong transferred hyperfine interaction (thfs) A^{19} exists between the Mn^{2+} and the nearest-neighbor (NN) ^{19}F nuclei. The study of this interaction is important because it is essential to the understanding of the ^{19}F nuclear relaxation in Mn:PbF_2 (Ref. 1) in the superionic region.

In the present work, the electron paramagnetic resonance (EPR) of Mn^{2+} in Mn^{2+}:PbF_2 was reexamined in an attempt to resolve an apparent contradiction between an earlier EPR study[3] above 77 K and an NMR investigation[5] below 2 K, in regard to the magnitude of $A_{||}^{19}$ and $A_{\perp}^{19}$, which are, respectively, the parallel and perpendicular components of the ^{19}F thfs relative to the Mn^{2+}–F^- bond axis. The previous EPR work exhibited a ^{19}F thfs spectrum which was not well resolved and was examined only with the field along the [100] direction of the crystal. As a result, only the quantity $[\frac{1}{3}(A_{||}^{19})^2+\frac{2}{3}(A_{\perp}^{19})^2]^{1/2}=25\pm1.5$ MHz was determined at $T=77$ K. The later NMR study below 2 K determined $A_{||}^{19}$ and $A_{\perp}^{19}$ separately from the observation of the resonance of nuclei of F^- ions which are NN to a Mn^{2+} impurity, by rotation of the external field in the (110) plane. The NMR was unobservable for $T>2$ K. A value of the quantity $[\frac{1}{3}(A_{||}^{19})^2+\frac{2}{3}(A_{\perp}^{19})^2]^{1/2}=35.6\pm0.01$ MHz was obtained at $T=1.5$ K. It was suggested that a possible misalignment of the crystal in the first experiment was responsible for the discrepancy between the two values.

The present work resolves this apparent discrepancy. It will be shown that our results for $A_{||}^{19}$ and $A_{\perp}^{19}$ are in agreement with the earlier EPR study from room temperature down to approximately 50 K, but at $T\simeq50$ K, the equilibrium positions of the ^{19}F nuclei NN to a Mn^{2+} change, bringing the values of $A_{||}^{19}$ and $A_{\perp}^{19}$ closer to those reported in the lower tempeature NMR experiment.

In Sec. II of this paper, we discuss the spin Hamiltonian appropriate to Mn^{2+} in Mn:PbF_2. Section III describes the experimental procedures, the observed EPR spectra, and their comparison with the theoretically expected ones. In Secs. IV and V we discuss the experimental results and the conclusions, respectively.

II. SPIN HAMILTONIAN

When introduced substitutionally for Pb^{2+} in β-PbF_2, the Mn^{2+} ion occupies the center of a cube formed by eight fluorines.[1,5] The spin Hamiltonian appropriate to this situation is[3]

$$\mathcal{H}=g\mu_B\mathbf{H}_0\cdot\mathbf{S}+A^{55}\mathbf{I}^{55}\cdot\mathbf{S}-\gamma^{55}\mathbf{H}_0\cdot\mathbf{I}^{55}+\sum_{j=1}^{8}\mathbf{S}\cdot\overleftrightarrow{\mathbf{A}}_j^{19}\cdot\mathbf{I}_j^{19}-\gamma^{19}\sum_{j=1}^{8}\mathbf{H}_0\cdot\mathbf{I}_j^{19}+\mathcal{H}_{\text{cub}}\,, \tag{1}$$

where $\mathbf{S}$, $\mathbf{I}^{55}$, $\mathbf{I}^{19}$, and $\mathbf{H}_0$ are the Mn^{2+} electronic spin ($S=\frac{5}{2}$), the ^{55}Mn nuclear spin ($I^{55}=\frac{5}{2}$), the ^{19}F nuclear spin ($I^{19}=\frac{1}{2}$), and the applied external field, respectively. The first term represents the electronic Zeeman energy, the next two the ^{55}Mn hfs and Zeeman interactions, the fourth and fifth terms the thfs interaction between the Mn^{2+} and ^{19}F spins, and the F^{19} nuclear Zeeman energy, respectively, with sums taken over the eight fluorines NN to the Mn^{2+}. The last term is the cubic crystal-field interaction, which is hereafter neglected because it gives rise to the negligible corrections to the values determined for the ^{19}F thfs parameters.[3] First, consider the effects of the ^{55}Mn hyperfine interaction on the EPR spectrum. At a constant frequency, the allowed electronic transitions $|M,m^{55}\rangle\rightarrow|M+1,m^{55}\rangle$ to third order in A^{55} occur at fields given by[4]

$$H=H_0-A^{55}m^{55}-[(A^{55})^2/2H_0][I^{55}(I^{55}+1)-(m^{55})^2-m^{55}(2M-1)]$$
$$-[(A^{55})^3/2H_0^2]\{(2M-1)[2I^{55}(I^{55}+1)-3(m^{55})^2]-m^{55}[S(S+1)+I^{55}(I^{55}+1)-2-(m^{55})^2]+3m^{55}M(M-1)\}\,, \tag{2}$$

where M and m^{55} are the quantum numbers for S_z and I_z^{55}, respectively, with $\hat{\mathbf{z}}$ the direction of the applied field.

The EPR spectrum will consist of six hyperfine lines split by the term $A^{55}m^{55}$. The terms second and third order in A^{55} depend on the electronic quantum number M, and thus give an additional "fine-structure" splitting to the m^{55} hfs. For the particular hyperfine component $m^{55}=\frac{1}{2}$, however, with the values $A^{55}=-95$ Oe and H_0 corresponding to the X band, the M dependence is accidentally smaller than it is for the other m^{55} components, and the additional fine-structure lines will be almost superimposed.

The effect of the ^{19}F thfs term is to further split the electronic transitions. Since $A^{55}\gg A^{19}$, the thfs will be superimposed on each ^{55}Mn hyperfine component. The $m^{55}=\frac{1}{2}$ hyperfine component alone will show a well-resolved thfs, without further splittings due to the M dependence. That part of the spin Hamiltonian which depends upon the ^{19}F nuclei may be written, for each nucleus, as

$$\mathcal{H}=\mathbf{S}\cdot\overleftrightarrow{\mathbf{A}}_j^{19}\cdot\mathbf{I}_j^{19}-\gamma^{19}H_0(\mathbf{I}_j^{19}\cdot\hat{\mathbf{z}})\ . \tag{3}$$

For sufficiently large H_0 we may express $\mathbf{S}\cdot\overleftrightarrow{\mathbf{A}}_j^{19}$ as $M\overleftrightarrow{\mathbf{A}}_j^{19}\cdot\hat{\mathbf{z}}$. The individual ^{19}F nuclei are then quantized along an effective magnetic field[6]

$$\mathbf{H}_{\rm eff}=H_0\hat{\mathbf{z}}-\frac{M}{\gamma^{19}}\overleftrightarrow{\mathbf{A}}_j^{19}\cdot\hat{\mathbf{z}}\ . \tag{4}$$

In ordinary EPR, the nuclear Zeeman energy is much smaller than the transferred hyperfine energy. In this case, the electronic transitions $|M\rangle\rightarrow|M+1\rangle$ do not change the direction of the effective field, and do not flip the ^{19}F nuclear spins. The allowed transitions are

$$|M,m^{55},m^{19}\rangle\rightarrow|M+1,m^{55},m^{19}\rangle\ . \tag{5}$$

The spectrum that results in this case has been called *simple*.[6]

When the nuclear Zeeman term and the transferred hyperfine interaction are comparable in magnitude, the electronic transitions may induce nuclear transitions $|m^{19}\rangle\rightarrow|m^{19}\pm1\rangle$. Let the unit vectors along the direction of the resultant field for the two electronic states be $\hat{\boldsymbol{\xi}}$ and $\hat{\boldsymbol{\eta}}$, respectively, and ϕ the angle between the two effective fields. If $|+\rangle$ and $|-\rangle$ are the initial states along $\hat{\boldsymbol{\xi}}$, the final states along $\hat{\boldsymbol{\eta}}$ are[7]

$$\begin{aligned}|+\rangle^f&=\cos(\tfrac{1}{2}\phi)|+\rangle+\sin(\tfrac{1}{2}\phi)|-\rangle\ ,\\ |-\rangle^f&=-\sin(\tfrac{1}{2}\phi)|+\rangle+\cos(\tfrac{1}{2}\phi)|-\rangle\ .\end{aligned} \tag{6}$$

The transition probabilities are given by r_i and s_i:

$$\begin{aligned}&|+\rangle\rightarrow|+\rangle^f \text{ and } |-\rangle\rightarrow|-\rangle^f\ ;\ s_i=\cos^2(\tfrac{1}{2}\phi)\\ &|+\rangle\rightarrow|-\rangle^f \text{ and } |-\rangle\rightarrow|+\rangle^f\ ;\ r_i=\sin^2(\tfrac{1}{2}\phi)\ .\end{aligned} \tag{7}$$

If the change in the field direction is $\phi\simeq0°$ or $\phi\simeq180°$, one pair of transitions will be almost inhibited; the resulting spectrum in this case is *simple*. On the other hand, a spectrum with significant contributions from both allowed and forbidden transitions is called *complex*.

$$\cos\phi=\frac{P(M)P(M-1)\cos^2\theta+Q(M)Q(M-1)\sin^2\theta}{[P^2(M)\cos^2\theta+Q^2(M)\sin^2\theta]^{1/2}[P^2(M-1)\cos^2\theta+Q^2(M-1)\sin^2\theta]^{1/2}}\ , \tag{8}$$

where θ is the angle between the applied field and the Mn^{2+}–F^- bond axis—a [111] direction of the crystal. $P(M)$ and $Q(M)$ are given by

$$\begin{aligned}P(M)&=MA_{\parallel}^{19}-\gamma^{19}H_0\ ,\\ Q(M)&=MA_{\perp}^{19}-\gamma^{19}H_0\ .\end{aligned} \tag{9}$$

The ^{19}F line positions and their intensities are obtained by the expansion of the following expression, for arbitrary x (Ref. 6):

$$\prod_{j=1}^{8}[r_j(x^{U_j}+x^{-U_j})+s_j(x^{V_j}+x^{-V_j})]\ , \tag{10}$$

where

$$\begin{aligned}U_j=\tfrac{1}{2}\{&[P^2(M)\cos^2\theta+Q^2(M)\sin^2\theta]^{1/2}\\ &+[P^2(M-1)\cos^2\theta+Q^2(M-1)\sin^2\theta]^{1/2}\}\end{aligned}$$

and

$$\begin{aligned}V_j=\tfrac{1}{2}\{&[P^2(M)\cos^2\theta+Q^2(M)\sin^2\theta]^{1/2}\\ &-[P^2(M-1)\cos^2\theta+Q^2(M-1)\sin^2\theta]^{1/2}\}\ .\end{aligned} \tag{11}$$

The exponents of x in this expansion give the field positions of the fluorine superhyperfine transitions, and the associated coefficients give the relative intensities. The intensities should also be multiplied by the proper factor for the relative intensities of the fine-structure lines,[8]

$$(5{:}8{:}9{:}8{:}5)\ . \tag{12}$$

It will be seen in Secs. III and IV that in our experiment the specific conditions necessary to observe a *complex* spectrum are satisfied below 50 K for $\mathbf{H}_0$ applied parallel to the [100] direction of the crystal. In all other cases, the spectrum will be *simple*, and the expressions for the field shift Z of the EPR due to the ^{19}F thfs can be reduced to

$$Z=\sum_{j=1}^{8}m_j^{19}[(A_{\parallel}^{19})^2\cos^2\theta_j+(A_{\perp}^{19})^2\sin^2\theta_j]^{1/2}\ . \tag{13}$$

When $\mathbf{H}_0$ is applied parallel to [100], $\theta_j=54.7°$ for all the eight NN ^{19}F nuclei,[8] and Z becomes

$$Z=m^{19}[\tfrac{1}{3}(A_{\parallel}^{19})^2+\tfrac{2}{3}(A_{\perp}^{19})^2]^{1/2}\ , \tag{14}$$

where $m^{19}\equiv\sum_{j=1}^{8}m_j^{19}$, and the ^{19}F thfs consists of nine lines, corresponding to the allowed m^{19} values. Since the splittings in this case are all equal, we denote them by z

and $Z = m^{19} z$.

If $\mathbf{H}_0$ is applied parallel to [110], there are two groups of four equivalent ^{19}F; one group has $\theta_j = 90°$,[8] for which

$$Z_1 = m_1^{19} A_\perp^{19} , \tag{15}$$

where m_1^{19} is the sum over the m_j's of the four ^{19}F.

The other group has $\theta_j = 35.3°$,[8] and

$$Z_2 = m_2^{19} [\tfrac{2}{3}(A_\parallel^{19})^2 + \tfrac{1}{3}(A_\perp^{19})^2]^{1/2} , \tag{16}$$

where m_2^{19} is the sum of the m_j's of these four ^{19}F. The ^{19}F thfs is obtained for $\mathbf{H}_0 \| [110]$ by adding (15) and (16), giving a total of 25 possible lines.

With $\mathbf{H}_0 \| [111]$ direction, there are two ^{19}F that have $\theta_j = 0°$ (Ref. 8), for which

$$Z_1 = m_1^{19} A_\parallel^{19} \tag{17}$$

and there are two groups of three ^{19}F having $\theta_j = 70.5°$ and $\theta_j = 109.5°$, respectively; for them,

$$Z_2 = m_2^{19} [0.111 (A_\parallel^{19})^2 + 0.688 (A_\perp^{19})^2]^{1/2} . \tag{18}$$

m_1^{19} and m_2^{19} are the sums of m_j over the first group of two and the second group of six ^{19}F, respectively.

The ^{19}F thfs is obtained for $\mathbf{H}_0 \| [111]$ by adding (17) and (18). The expressions for the resonant fields $\mathbf{H}_0$ given above were used to generate the computer spectra to compare with the experimental results of Sec. III.

III. EXPERIMENTAL PROCEDURES AND RESULTS

We have measured the X-band EPR of Mn^{2+} in Mn:PbF_2 with a Bruker EPR spectrometer. The data were averaged and recorded with a Nicolet model No. 1270 Instrument Computer. The sample was a β-PbF_2 crystal, with a concentration $c = 0.015$ mol % of Mn^{2+}. It was oriented using standard x-ray diffraction techniques.

$\mathbf{H}_0$ was applied in the (110) plane, perpendicular to the axis of rotation. The [100], [110], and [111] directions were found by rotating the sample and looking for intensity maxima in the EPR spectrum. The temperature was measured with a chromel versus Fe:Au thermocouple with the temperature difference between the thermocouple and the sample in the resonant cavity no more than 1 K. The modulation field used was 0.8 Oe.

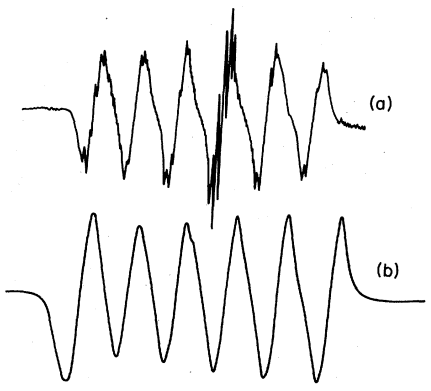

FIG. 1. Observed EPR spectrum of Mn^{2+} ($c = 0.015^{m/0}$) in Mn:PbF_2 for $\mathbf{H}_0 \| [100]$ at (a) $T = 293$ K and (b) $T = 6$ K.

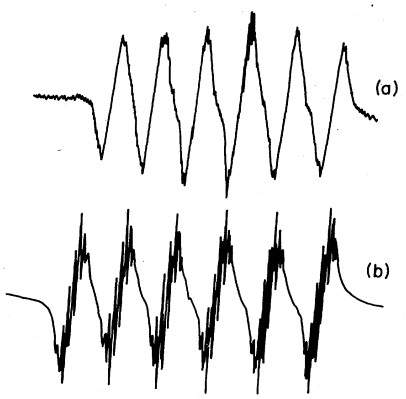

FIG. 2. Observed EPR spectrum of Mn^{2+}, for $\mathbf{H}_0 \| [110]$, at (a) $T = 293$ K and (b) $T = 6$ K.

The observed, small field modulation, derivative EPR spectrum of Mn^{2+} in Mn:PbF_2 is shown in Fig. 1 with $\mathbf{H}_0 \| [100]$, at room temperature and $T = 6$ K [Figs. 1(a) and 1(b)], respectively, and in Fig. 2 with $\mathbf{H}_0 \| [110]$ at the same two temperatures [Figs. 2(a) and 2(b)]. In both cases, we see that the thfs in the room-temperature data is sharpest and best resolved on the $m^{55} = \frac{1}{2}$ component, because of the near cancellation of the m dependence of the second- and third-order ^{55}Mn hfs on this line, as mentioned above. All other m^{55} components are more severely broadened. Between $T = 77$ K and $T = 6$ K several dramatic changes occur. In the [100] data, the sharp thfs nearly disappears from the $m^{55} = \frac{1}{2}$ line, while in the [110] data, the thfs becomes much sharper and better resolved, and appears equally on *all* m^{55} components.

The evolution of the ^{19}F thfs superimposed on the particular Mn^{2+} hfs component $m^{55} = \frac{1}{2}$ is shown in Figs. 3 and 4 for $\mathbf{H}_0 \| [100]$ and $\mathbf{H}_0 \| [110]$, respectively, for different temperatures. In these figures the upper spectra (a)

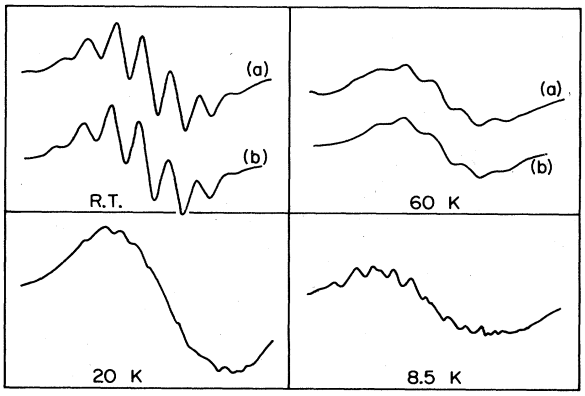

FIG. 3. thfs observed on the $m^{55} = \frac{1}{2}$ component of the EPR spectrum for $\mathbf{H}_0 \| [100]$, at different temperatures. (a) Observed; the gains used are 3.2×10^5, 5×10^4, 5×10^4, and 3.2×10^4 for room temperature, 60, 20, and 8.5 K, respectively. (b) Computer simulated, using Eq. (14) and the parameters listed in Table I.

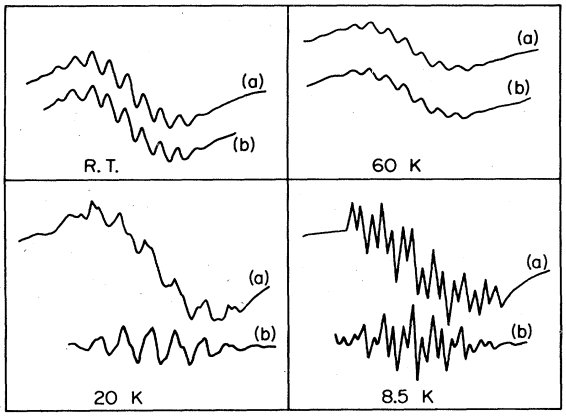

FIG. 4. thfs observed on the $m^{55}=\frac{1}{2}$ component of the EPR spectrum for $\mathbf{H}_0||[110]$, at different temperatures. (a) Observed; the gains are the same as in Fig. 3. (b) Computer simulated, using Eqs. (15) and (16), and the parameters listed in Table II.

are the experimental ones, and the lower (b), the computer-generated simulations, which will be discussed in the following section. Between room temperature and $T=60$ K, the thfs for both orientations is seen to broaden and weaken somewhat, but otherwise there is no change in the spectra. At $T=20$ K, both spectra have changed, but are not well resolved. At $T=8.5$ K, the [100] spectrum appears to be very complicated: Many sharp lines are visible, but no regular pattern is apparent. The [110] data, however, show a new, quite different resolved structure.

IV. ANALYSIS OF THE EXPERIMENTAL RESULTS

In the analysis of the results, the following three temperature regions can be distinguished.

(a) High-temperature region: 50 < T < 300 K. The thfs that is superimposed on the Mn^{2+} hyperfine components other than the $m^{55}=\frac{1}{2}$ is split by the fine structure, indicating that in this temperature region all of the electronic transitions are observed. All of these transitions are essentially purely "allowed," except for the $|\frac{1}{2}\rangle\rightarrow|-\frac{1}{2}\rangle$ one, which is complex, having significant probabilities for both allowed and forbidden transitions. However, the observed spectrum is the sum of the five electronic transitions with relative intensities given by (12). The complex $|\frac{1}{2}\rangle\rightarrow|-\frac{1}{2}\rangle$ transition, with relative weight of only $\frac{9}{35}$, is not seen, and the spectrum appears to be simple.

For $\mathbf{H}_0||[100]$ the thfs at room temperature is found to be indistinguishable from a simple 9-line spectrum as shown in Fig. 3(b). The value of $z=24$ MHz required to fit the data at $T=293$ and 60 K (Table I) agrees quite well with the value previously measured at $T=77$ K (see Table III).

For $\mathbf{H}_0||[110]$, the spectrum is also indistinguishable from a simple one. For the ratio $A_{||}^{19}/A_{\perp}^{19}=2.43$, many of the 25 lines given by Eqs. (15) and (16) overlap, giving a 13-line spectrum. The values of $A_{||}^{19}$ and $A_{\perp}^{19}$ used in the simulation are shown in Table II. The best values of z, $A_{||}^{19}$, and $A_{\perp}^{19}$ which simultaneously fit both the [100] and [110] data are shown in Table III. In all cases, Gaussian line profiles were found to give the best agreement between experiment and the simulations, with widths indicated in Tables I and II. The thfs observed is consistent with local cubic symmetry around the Mn^{2+}, but the linewidths broaden as the temperature is lowered.

TABLE I. Parameters determined from the best fit to the computer simulations of Eq. (14) for different temperatures for $\mathbf{H}_0||[100]$.

T (K)	z (MHz)	ΔH_{pp} (Oe)
293	24	7.5
60	24	10

(b) Intermediate region: 20 < T < 50 K. A broad background is observed added to the thfs in this temperature region, and the thfs is not resolved. This we attribute to the beginnings of a random crystal distortion, which produces the background observed and ultimately results in substantial changes in the values of $A_{||}$ and $A_{\perp}$ at $T<20$ K.

(c) Low-temperature region: T<20 K. The ^{19}F thfs with $\mathbf{H}||[110]$ is identical for all of the m^{55} components, including the $m^{55}=\frac{1}{2}$. This implies no M-dependent splitting, which can be true if only the $M\rightarrow M-1$ transition is present, as shown by Eq. (2). The intensities of the ^{19}F thfs are reduced, after corrections for T, to $\frac{9}{35}$ of the corresponding intensities at room temperature, indicating that the only transition observed is $|\frac{1}{2}\rangle\rightarrow|-\frac{1}{2}\rangle$.

What has happened to the remaining outer electronic transitions? We believe that they are broadened by random crystal distortions, and only contribute to the observed background for $T<50$ K. The perturbing Hamiltonian represented by an axial or orthorhombic distortion[4] affects the outer electronic transitions (i.e., $|\pm\frac{5}{2}\rangle\leftrightarrow|\pm\frac{3}{2}\rangle$ and $|\pm\frac{3}{2}\rangle\leftrightarrow|\pm\frac{1}{2}\rangle$) to *first order* in D/H, where D is the axial field distortion and H is the applied field, but the $|\frac{1}{2}\rangle\rightarrow|-\frac{1}{2}\rangle$ transition is affected only to *second order* in D/H. If D were the same at all sites of the crystal, the transitions would be just shifted in frequency. However if D is random in magnitude and direction, the spectrum would be homogeneously broadened as is observed.

The spectrum observed for $\mathbf{H}||[100]$ is extremely complicated and essentially unresolved because it is *complex*. Only the $|+\frac{1}{2}\rangle\rightarrow|-\frac{1}{2}\rangle$ transition is seen at low T, which is the one with appreciable "forbidden" intensity.

TABLE II. Parameters determined from the best fit to the computer simulations of Eqs. (15) and (16) for $\mathbf{H}_0||[110]$ and Eqs. (17) and (18) for $\mathbf{H}_0||[111]$, for different temperatures.

Direction	T (K)	$A_{||}$ (MHz)	$A_{\perp}$ (MHz)	ΔH_{pp} (Oe)
[110]	293	36	14.85	5.5
	60	36	14.85	6
	20	39.2	26	3.4
	8.5	46.2	26	3
[111]	8.5	46.2	26	5

TABLE III. The best values of $A_{\parallel}^{19}$, $A_{\perp}^{19}$, and z, as determined by fitting the spectra in the [100] and [110] directions simultaneously, for different temperatures, and their comparison with those obtained in Refs. 3 and 5.

Reference	T (K)	$A_{\parallel}^{19}$ (MHz)	$A_{\perp}^{19}$ (MHz)	z (MHz)
This experiment	$50<T<293$	36±0.5	14.8±0.5	24.1±0.3
Measured in Ref. 3	77			25±1.5
This experiment	20	39.2±1.5	26±1.5	31.0±0.3
This experiment	4.5	46.2±1.5	26±1.5	34±1
Measured in Ref. 4	2	49.58±0.02	26.04±0.01	35.6±0.01

Using Eqs. (7) and (8), we find $r=0.86$ and $s=0.14$, using the parameters determined from the $\mathbf{H}_0||[110]$ data. These probabilities result in appreciable intensities for an extremely large number of closely spaced lines, as seen in the data. No attempt at fitting the spectrum has been made.

For $\mathbf{H}_0||[110]$, the four ^{19}F with $\theta_j=90°$ give a 5-line spectrum of purely allowed transitions. For the other four, with $\theta_j=35.3°$, the transition probabilities are found to be $r_i=0.95$, $s_i=0.05$. Thus the spectrum is close enough to simple that the forbidden lines are not seen. For the ratio $A_{\parallel}^{19}/A_{\perp}^{19}=1.78$, several lines of the 25-line spectrum overlap, resulting in a fairly simple spectrum of 19 lines, the outer two of which are much weaker than the others, and are not seen. The simulation in Fig. 4 nicely reproduces the sharp part of the experimental spectrum. The parameters obtained for the best fits to the data are given in Tables II and III. The broad background in the data presumably arises from broadened transitions other than $|\frac{1}{2}\rangle\rightarrow|-\frac{1}{2}\rangle$.

The thfs shows that the local symmetry is still nearly cubic. The values of $A_{\parallel}^{19}$ and $A_{\perp}^{19}$ obtained, shown in Table III, agree reasonably well with those measured by Vernon and King at 2 K but differ substantially from those at higher T. The symmetric part of the hyperfine interaction can be expressed as[5]

$$A_s^{19}=(2A_{\perp}^{19}+A_{\parallel}^{19})/3\ . \tag{19}$$

Figure 5 shows the measured temperature dependence of A_s^{19}. If A_s^{19} is assumed to be proportional to r^{-6}, where r is the impurity-ligand distance,[9,10] then the change in A_s^{19} at 50 K implies a 6% reduction in r. But neutron scattering experiments[11,12] show there is no anomalous temperature dependence of the lattice constant in pure PbF_2, and that, between room-T and 50 K, r is only reduced by 0.6%, because of thermal expansion. Thus the change in A cannot be explained simply on the basis of thermal expansion, namely anharmonic effects. Nor can the harmonic vibrations of the lattice cause A_s^{19} to *decrease* at high temperatures—in fact just the opposite would be the case.[13]

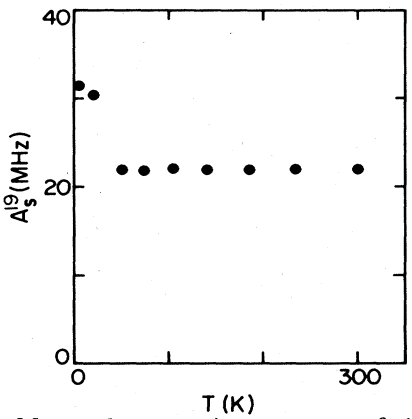

FIG. 5. Measured symmetric component of the hyperfine tensor, A_s^{19}, as a function of temperature. Note the abrupt change in A_s^{19} that occurs in the region around 50 K.

A likely explanation is that a local *contraction* of the Mn^{2+}-F nearest neighbor separation occurs upon cooling below 50 K and this manifests itself in two ways. First, the ^{19}F thfs interaction *increases* as T decreases and second the strain caused by the local distortion results in a propagating strain field which in turn produces a random axial (and/or orthorhombic) crystal field. The latter broadens all EPR transitions except the $|\frac{1}{2}\rangle\leftrightarrow|-\frac{1}{2}\rangle$ to first order in D.

V. SUMMARY AND DISCUSSION

The comparison between our experimental results for $A_{\parallel}^{19}$, $A_{\perp}^{19}$, and z, and those previously reported[3,4] is given in Table III. Our high-T results are seen to agree with the earlier EPR measurements at 77 K and the low-T ones agree with the NMR measurements made below 2 K. This resolves the earlier apparent discrepancy between the EPR and NMR measurements.

Vernon and King[5] did observe evidence of line broadening in their 2-K experiment. The NMR signal of the ^{19}F nuclei NN to a Mn^{2+} ion appeared to be inhomogeneously broadened, with the broadening very angularly dependent. When the magnetic field H_0 was applied parallel or perpendicular to [111], broadening was at a minimum and approximately 50 Oe. In these positions, the field positions of the NMR lines are given by $A_{\parallel}^{19}$ and $A_{\perp}^{19}$, respectively. The broadening was attributed to a distribution of the parameters as might result from a distribution of Mn-F distances.[5]

What can be the origin of the distortion? Samara[14] investigated the dielectric properties of PbF_2. He found an anomalous temperature dependence and a large value of the real part of the dielectric constant ϵ', which he associated with a soft, long-wavelength, transverse-optical phonon. He suggested that PbF_2 was an incipient ferroelec-

tric, with a negative T_c. We believe that this soft mode might be related to the observed crystal distortion in that it implies a sensitivity of the crystal to distortions. This distortion is probably a consequence of the smallness of the ionic radius of the Mn^{2+} (0.80 Å), relative to that of Pb^{2+} (1.2 Å). It would be of considerable interest to investigate the temperature dependence of the transverse-optical mode to see if it correlates with the results of the present experiment.

ACKNOWLEDGMENTS

One of the authors (M.M.) would like to thank Mr. Fernando Moraes, Dr. Jorg Kotthaus, Dr. Richard McCall, and Mr. Howard Schaeffer for their interest and help. We are thankful to Mr. Neil Nighman for the preparation of the samples. The early stages of this research were supported in part by the U.S. Department of Energy under Grant No. DE-AT03-76ER70244.

[1]S. P. Vernon, P. Thayamballi, R. D. Hogg, D. Hone, and V. Jaccarino, Phys. Rev. B **24**, 3756 (1981).

[2]M. Madrid, A. R. King, and V. Jaccarino (unpublished).

[3]C. Evora and V. Jaccarino, Phys. Rev. Lett. **39**, 1554 (1977); C. Evora, Ph.D. thesis, University of California at Santa Barbara, 1978 (unpublished).

[4]J. Shinar and V. Jaccarino, Phys. Rev. B **27**, 4034 (1983).

[5]S. P. Vernon and A. R. King, Phys. Rev. B **24**, 3772 (1981).

[6]A. M. Clogston, J. P. Gordon, V. Jaccarino, M. Peter, and L. R. Walker, Phys. Rev. **117**, 1222 (1960).

[7]U. Ranon and James S. Hyde, Phys. Rev. **141**, 259 (1966).

[8]R. J. Richardson, Sook Lee, and T. J. Menne, Phys. Rev. B **4**, 3837 (1971).

[9]G. B. Benedek and T. Kushida, Phys. Rev. **118**, 46 (1960).

[10]K. N. Shrivastava, Phys. Rev. B **20**, 2634 (1979).

[11]M. H. Dickens, W. Hayes, and M. T. Hutchings, J. Phys. (Paris) Colloq. **37**, C7-353 (1976).

[12]M. H. Dickens and M. T. Hutchings, J. Phys. C **11**, 461 (1978).

[13]E. Dormann, D. Hone, and V. Jaccarino, Phys. Rev. B **14**, 2715 (1976).

[14]G. A. Samara, Phys. Rev. B **13**, 4529 (1976).